Hot Deformation Behavior and Dynamic Recrystallization Model of 6082 Aluminum Alloy in High Temperature

Weiwei Ren [a,*], Chunguo Xu[b] and Xianglong Chen[c]

No.18, Xueqing Road, Haidian District, Beijing, China
Email: [a]renweiwei2009@126.com, [b]13910082751@163.com,
[c]chxlcorp2018@163.com

Abstract. By high temperature compression experiment, true stress vs true strain curve of 6082 aluminium alloy are obtained at the temperature 460°C -560°C and the strain rate 0.01s-1-10s-1. The effects of deformation temperature and strain rate on the grain evolution are investigated; Critical strain of dynamic recrystallization of 6082 aluminium alloy model is obtained. The results show lower strain rates are beneficial to increase the volume fraction of recrystallization, the average grain size is coarse; High strain rates are beneficial to refine average grain size, the volume fraction of dynamic recrystallization is less than that in low strain rates. High temperature cause coarse grains. Dynamic recrystallization grain evolution model and model of DRX fraction can effectively predict recrystallization grain size and recrystallization fraction of 6082 aluminium alloy thermal deformation.

1. Introduction

Dynamic recrystallization (DRX) plays an important role in grain size after metal thermal forming. It not only can fine grains, but also control mechanical properties [1].It is now recognized as a powerful tool to control the structure and properties of metals under industrial processing operations [2]. Data of deformation such as stress and strain can be obtained by Gleeble thermal simulation experiment under constant temperature and strain rates. Grain size of dynamic recrystallization can be investigated by EBSD. Study of the relationship between the deformation parameters and the microstructure evolution is of great significance for controlling the properties of the material.

Deformation temperature and strain rate are two important deformation parameters of materials. The relationship between flow stress and strain is established through $\sigma - \varepsilon$ curve. The occurrence of DRX is indicated by the appearance of a peak in the stress –strain curve. However, DRX is actually initiated before the strain corresponding to the peak stress. This threshold strain is known as the critical strain [3] [4]. The difficulty is how to control the grain size. The grain size of the forging surface is coarse, which is three hundred times or more large than that of the inner grains. Guo H L et al [5] obtained the model of the dynamic recrystallization of 7075 aluminum alloy through the compression test and simulated the dynamic recrystallization process by Finite Element Method (FEM),the result show the model was verified; Chen X H et al [6] studied the effect of temperature and strain rates on microstructure of 7085 aluminum alloy in high temperature and investigated the critical strain model; Shi L et al [7] researched on critical strain model and results indicate model is in good agreement with the experiment. The dynamic recrystallization behavior of various aluminum alloy materials has been studied widely. At present there are few studies on the dynamic recrystallization of 6082 aluminum alloy.

The stress-strain curves were obtained based on thermal compression experiment of the 6082 aluminum alloy. According to the experimental data of EBSD, recrystallized grain evolution and

dynamic recrystallization fraction distribution is researched. The process of dynamic recrystallization can be simulated by FEM base on the experimental data which will be helpful to better control the internal microstructure and mechanical properties of the 6082 aluminum alloy.

2. Experimental procedure

The chemical composition(wt.%) of 6082 aluminum alloy is 0.93Si,0.165Fe,0.056Cu, 0.454Mn,0.65Mg, 0.117Cr, 0.002Zn, 0.03Ti, The initial average grain size is 60 μm. The specification of raw materials is Φ30 mm×1000 mm, compressed specimens are machined to dimension Φ10 mm×15 mm, both the surface are perpendicular to the axis, the axis is parallel to the compression direction. The forming temperature is 460 ℃, 500 ℃, 540 ℃, 560 ℃ and the strain rate is 0.01 s^{-1}, 0.1 s^{-1}, 1 s^{-1}, 10 s^{-1}. The operation model of the thermal simulator is Gleeble-3500, heating speed of 1 ℃ s^{-1}, the specimens are heat preserved for three minutes when up to the set temperature. After the compression is finished, specimens are immediately quenched in water to retain the deformed microstructure. The compressed specimens are sectioned along the axial direction, microstructure is characterized by electro-polishing of the specimens for 10 seconds with voltage 20 V and current 1 A in a solution consisting of 10% perchloric acid and 90% ethanol. By EBSD observation of the internal microstructure, it is grain disorientation greater than or equal to 10° that distinguish the grain boundaries. On account of detection limitation in microstructure [8], the grain disorientation less than 3 degrees is not considered.

3. Results and discussions

3.1. Stress-strain curves

The true stress-true strain curves of 6082 aluminum alloy deformed at different temperatures and strain rates are shown in Figure 1. It is seen that the flow stress is increased with increasing strain rate and decreasing temperature. When the strain rates are 0.01 s^{-1} and 0.1 s^{-1}, all the flow curves exhibit a peak and then follow by gradual fall to a steady stress state which is indicative of the occurrence of DRX [9]. In the steady state, the hardening and the softening due to DRX are in a state of balance, flow stress almost remain the same with the increase of deformation. When the strain rates are $1s^{-1}$ and $10s^{-1}$, stress-strain curves are in fluctuation. Stress peaks and troughs appears alternately, which shows that the working hardening and the dynamic recrystallization take the dominant position alternately.

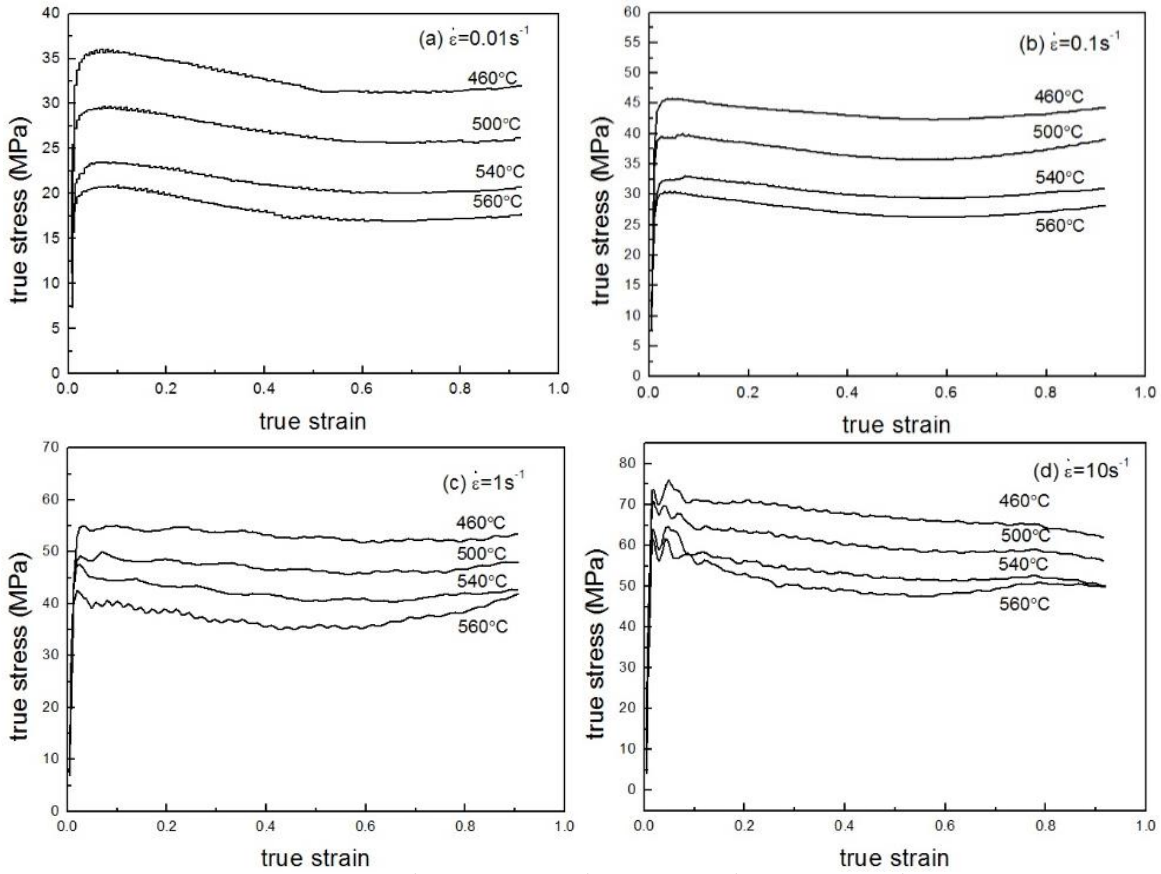

(a)$\dot{\varepsilon} = 0.01$ s^{-1} (b) $\dot{\varepsilon} = 0.1$ s^{-1} (c) $\dot{\varepsilon} = 1$ s^{-1} (d) $\dot{\varepsilon} = 10$ s^{-1}.

Figure 1. True stress-strain curves of 6082 Al-Si-Mg aluminum ally at different strain rates.

3.2. Stress-strain constitutive equations

The Arrhenius equation, which is widely accepted to describe the hot deformation behavior of alloy [10], gives approximations between Zener−Holloman parameter and flow stress σ. This theory can be expressed as in equation (1) ~ (3):

$$Z = \dot{\varepsilon} e^{Q/(RT)} \tag{1}$$

$$\dot{\varepsilon} = AF(\sigma) e^{Q/(RT)} \tag{2}$$

$$F(\sigma) = \begin{cases} \sigma^{n_1}, \alpha\sigma < 0.8 \\ e^{\beta\sigma}, \alpha\sigma > 1.2 \\ [\sinh(\alpha\sigma)]^n, \text{for all } \sigma \end{cases} \tag{3}$$

σ is the flow stress at a given strain (MPa);ε is the strain rate (s^{-1}); Q is the activation energy of hot deformation (kJ mol^{-1}); T is the thermodynamic temperature (K); R is the mole gas constant (8.314 J (mol K)$^{-1}$); α, β and n_1 are material constants with the relationship $\alpha=\beta/n_1$.

Based on the Figure 2(a) and Figure 2(b), the values β and n_1 are evaluated, β and n_1 are taken as the average value of the slopes of the $\ln\dot{\varepsilon} - \sigma$ curve and $\ln\dot{\varepsilon} - \ln\sigma$ curve.

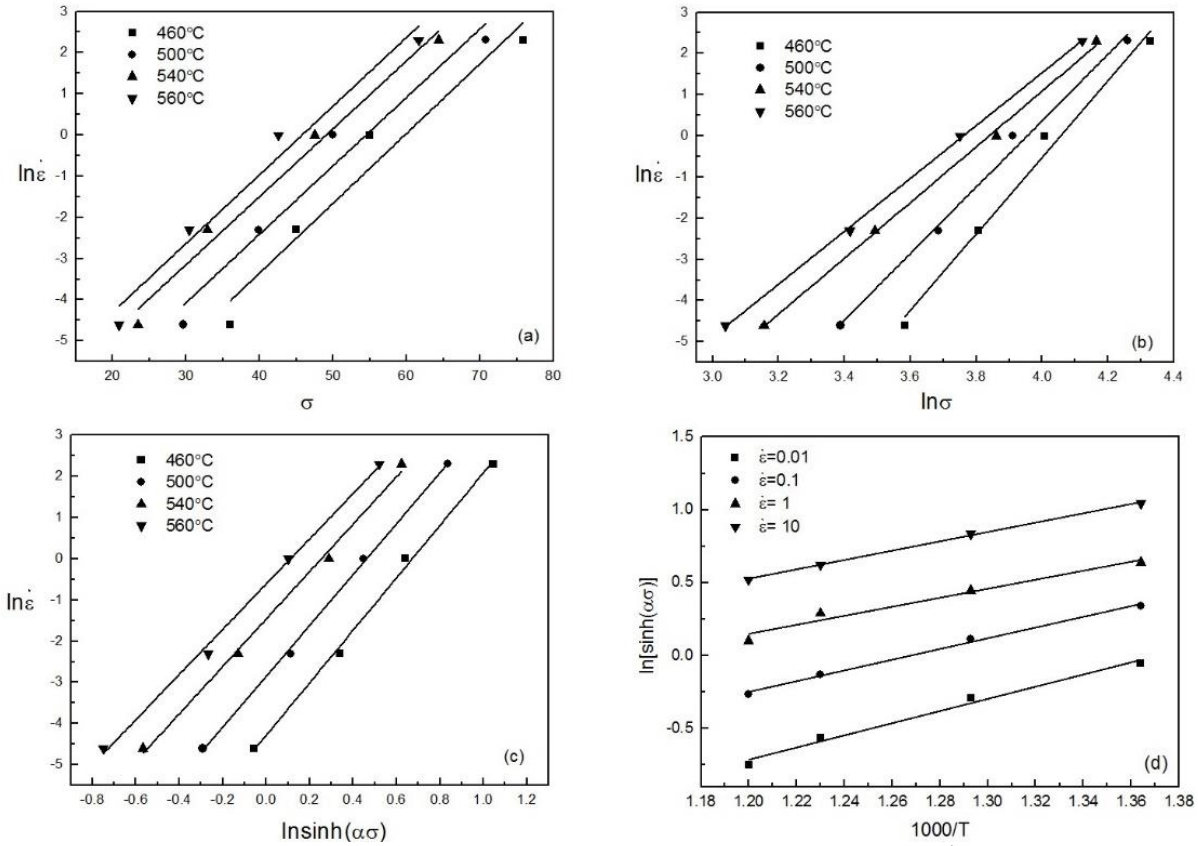

(a) $\ln\dot{\varepsilon} - \sigma$; (b) $\ln\dot{\varepsilon} - \ln\sigma$;(c) $\ln\dot{\varepsilon} - \ln\sinh(\alpha\sigma)$; (d) $\ln\dot{\varepsilon} - T^{-1}$.

Figure 2. Linear relationships of various parameters of 6082 aluminum alloy:

Activation *Q* can be calculated as follows:

$$Q = R\left(\frac{\partial \ln\dot{\varepsilon}}{\partial \ln[\sin(\alpha\sigma)]}\right)_T \left[\frac{\partial \ln[\sinh(\alpha\sigma)]}{\partial(1/T)}\right]_{\dot{\varepsilon}} \tag{4}$$

The Figure 2(c) and Figure 2(d) illustrates the relationships among $\ln\dot{\varepsilon}$, $\ln[\sin(\alpha\sigma)]$ and T^{-1}.

According to the above equation and figure 2, the material constants are listed in table 1.

Table 1. Material constants of 6082 aluminum alloy.

$\alpha(\mathrm{MPa}^{-1})$	n	$A(s^{-1})$	$Q(\mathrm{kJ}\cdot\mathrm{mol}^{-1})$
0.0269	5.89	4.36×10^{10}	174.9

So the mathematic model for stress of 6082 Al-Si-Mg alloy is summarized as follows:

$$\sigma = 37.2\ln\left\{\left(\frac{Z}{4.36\times10^{10}}\right)^{\frac{1}{5.89}} + \left[\left(\frac{Z}{4.36\times10^{10}}\right)^{\frac{2}{5.89}} + 1\right]^{\frac{1}{2}}\right\} \tag{5}$$

$$Z = \dot{\varepsilon}e^{\frac{174.9}{8.31T}} \tag{6}$$

3.3. Effect of deformation parameters on microstructure

The Figure 3 is EBSD image of grain structure when the temperature 540 ℃, true strain 0.6 and the strain rate $0.01s^{-1}$, $0.1s^{-1}$, $1s^{-1}$, $10s^{-1}$, Corresponding parameters ln*Z* is 21.3, 23.6, 25.9and 28.2.

Red line is grain boundary. Dynamic recrystallization occurs at temperature 540 ℃ and different strain rates from photographs, average grain size of recrystallized grains decreases with the increase of strain rate. It is also conducted that the gains are relatively small under the conditions of high *Z*.

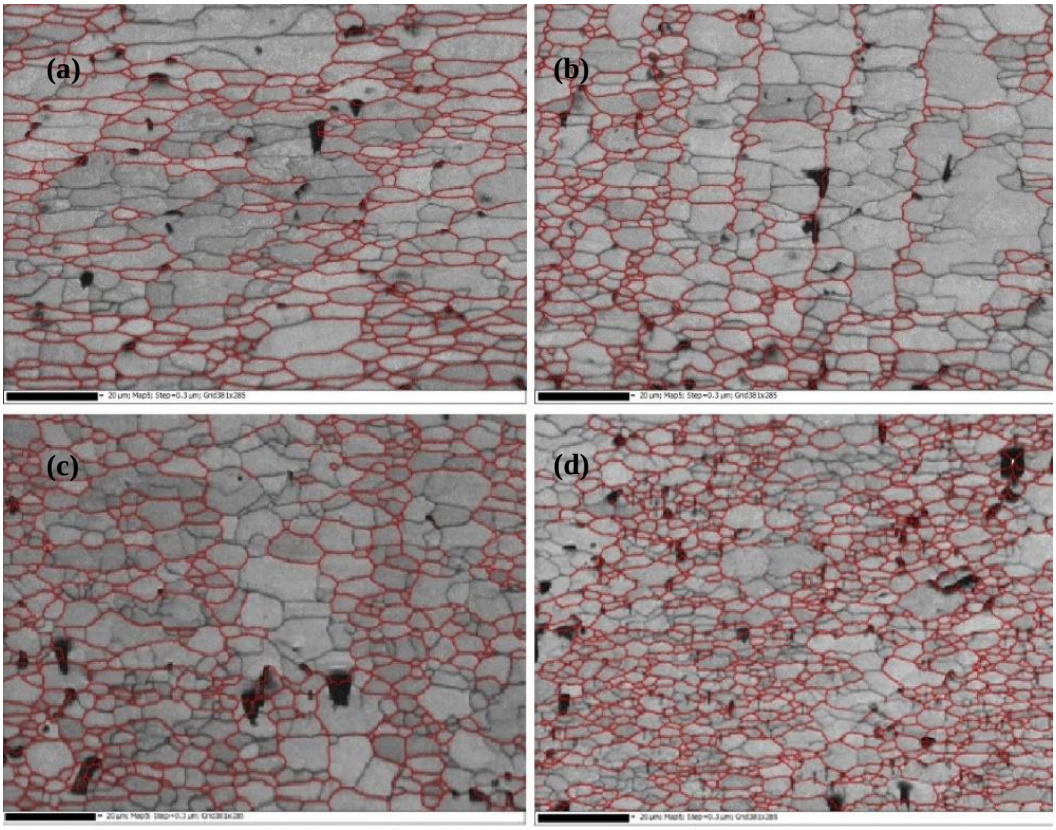

(a) $\dot{\varepsilon} = 0.01s^{-1}$(ln*Z*=21.3); (b) $\dot{\varepsilon} = 0.1s^{-1}$(ln*Z*=23.6)
(c) $\dot{\varepsilon} = 1s^{-1}$(ln*Z*=25.9); (d) $\dot{\varepsilon} = 10s^{-1}$(ln*Z*=28.2)

Figure 3. EBSD grain structure of 6082 aluminum alloy at different strain rates:

The Figure 4 is EBSD image of recrystallization volume fraction when the temperature 540 ℃, true strain 0.6 and the strain rate 0.01 s^{-1}, 0.1 s^{-1}, 1 s^{-1}, 10 s^{-1}, blue represents dynamic recrystallization region. Based on the data from EBSD post-processing software, the recrystallization volume fraction in (a)(b)(c)(d)are 78%, 60.3%, 67.8%, 69%. At lower strain rate, the dynamic recrystallization process is adequate, and the recrystallized grains have enough time to grow up (Figure 4 (a) (b)). The dynamic recrystallization of materials is closely related to the deformation time, and the deformation time at high strain rate is short, and the dynamic recrystallization will be limited. The recrystallization volume fraction is decreased with the increase of strain rates or ln*Z*.

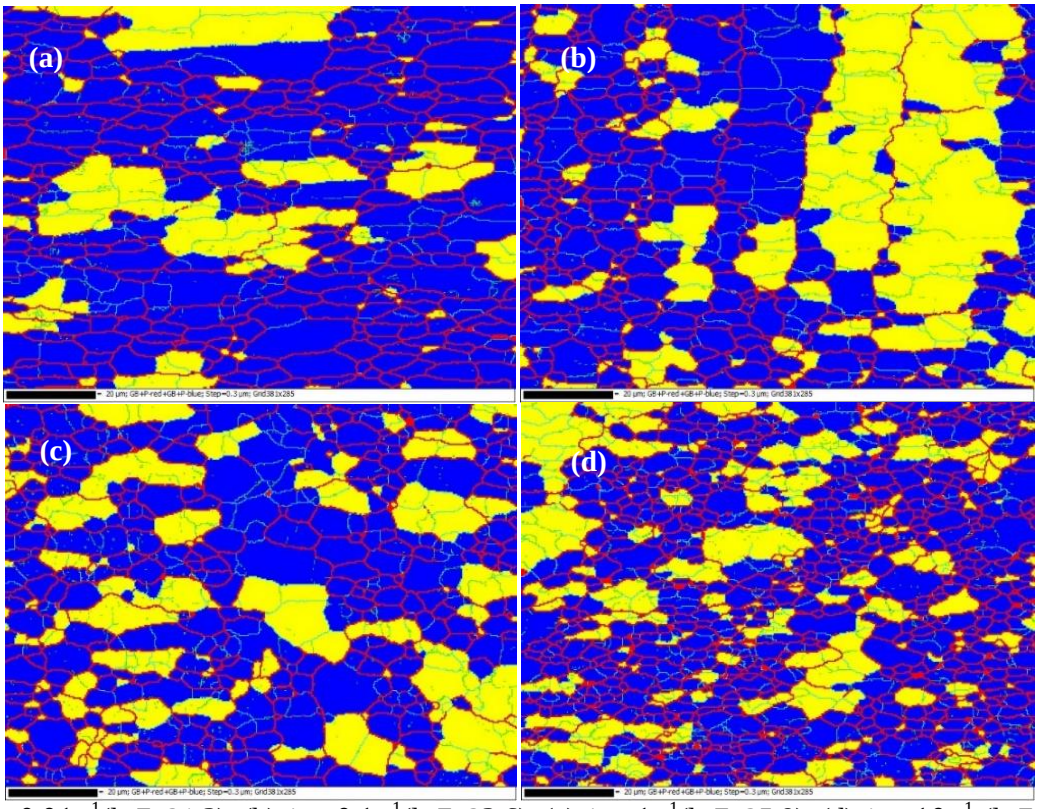

(a) $\dot{\varepsilon} = 0.01s^{-1}$(ln$Z$=21.3); (b) $\dot{\varepsilon} = 0.1s^{-1}$(ln$Z$=23.6); (c) $\dot{\varepsilon} = 1s^{-1}$(ln$Z$=25.9); (d) $\dot{\varepsilon} = 10s^{-1}$ (ln$Z$=28.2)

Figure 4. Recrystallization volume fraction of 6082 aluminum alloy at different strain rates:

The results from grain evaluation and recrystallization volume fraction evaluation reveals that high strain rates will refine grains and low strain rates is beneficial to improve the fraction of dynamic recrystallization when temperature keep the same.

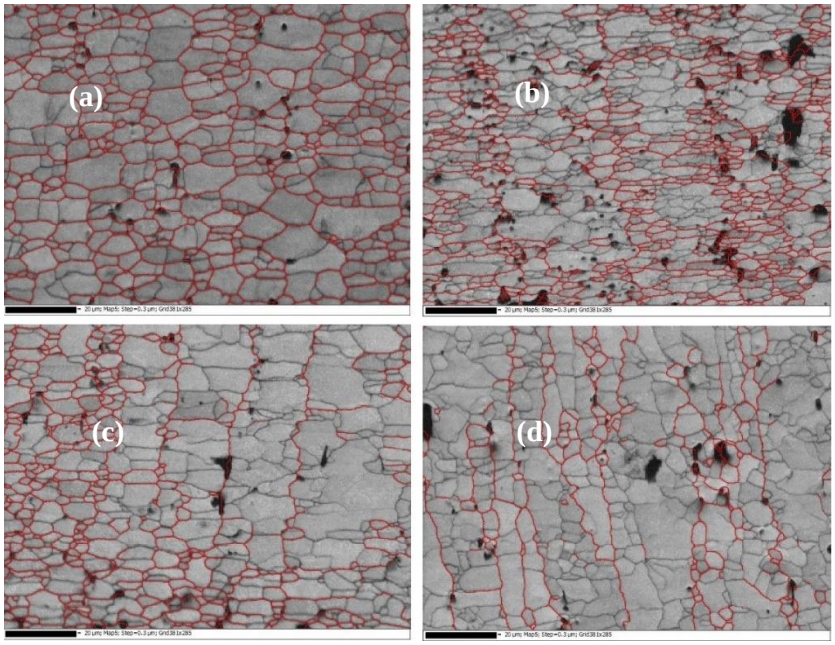

(a)460 ℃ (ln$Z$=26.4); (b)500 ℃ (ln$Z$=25); (c)540 ℃ (ln$Z$=23.6); (d)560 ℃ (ln$Z$=23).

Figure 5. EBSD grain structure of 6082 aluminum alloy at different temperatures:

The Figure 5 is EBSD image of grain structure when the strain rate is $0.1s^{-1}$, true strain 0.6 and the temperature is 460 ℃, 500 ℃, 540 ℃, 560 ℃, Corresponding parameters ln$Z$ is 26.4, 25, 23.6and 23. Red line is grain boundary. Dynamic recrystallization occurs at strain rate $0.1s^{-1}$ and different temperatures from photographs. At lower temperatures recrystallization grains are equiaxed grains (Figure 5(a)(b)), which gradually transform to columnar grains as the equiaxed grains grow up to annex the small grains (Figure 5(c)(d)).Average grain size of recrystallized grains increases with the increase of deforming temperature.

With the increase of deforming temperature, the movement of recrystallized grain boundary enhance. High temperature reduces dislocation density and hinders dynamic recrystallization nucleation. As is shown in Figure 6(d), blue represents dynamic recrystallization region.

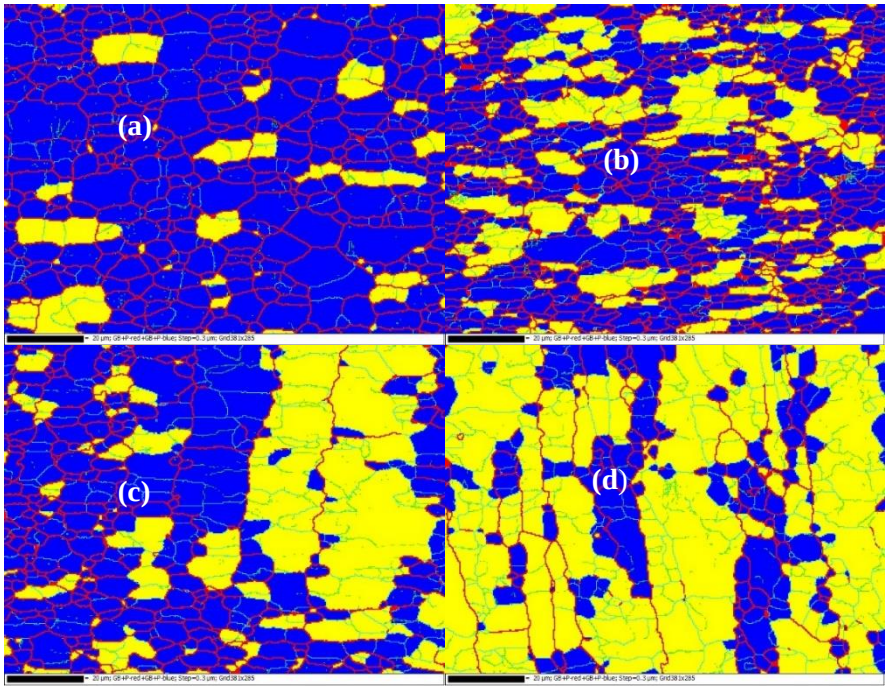

(a)460 ℃ (lnZ=26.4); (b)500 ℃ (lnZ=25); (c)540 ℃ (lnZ=23.6); (d)560 ℃ (lnZ=23).

Figure 6. Recrystallization volume fraction of 6082 aluminum alloy at different strain rates:

From the Figure 6 above, the deformation keeps similar, amount of recrystallization volume fraction increase as deformation temperature decrease at a given strain rate. The higher the deformation temperature, the smaller recrystallization volume fraction of the dynamic recrystallization. It is also shown that the dynamic recrystallization fraction decrease with the decrease of ln$Z$

3.4. Dynamic recrystallization model of 6082 aluminium alloy

When the mental begins to recrystallize dynamically in thermal deformation, the dynamic recrystallization model including peak strain equation, critical strain equation, dynamic recrystallization kinetic equation and the recrystallization grain size equation. All the equations can be expressed in terms of the follows [11]:

$$\mathrm{D_{drex}} = \mathrm{CZ^{a}} \tag{7}$$

$$\varepsilon_{\mathrm{p}} = \mathrm{Ad_0{}^{p}Z^{q}} \tag{8}$$

$$\varepsilon_{\mathrm{c}} = \alpha\varepsilon_{\mathrm{p}} \tag{9}$$

ε_c: the critical strain when material begins to recrystallization dynamically;ε_p:peak strain; D_{drex}:DRX grain size; d_0 : the origin grain size; A,p,q,k,n,C and α :material constants;Z:Zener-Hollomon parameters; X: the fraction of DRX.

According the compression experiment data, the relationships between ε_c , ε_p and Z is plot in Figure 8, So α≈(0.678~0.707).In subsequent calculation, α is taken as the average values 0.69.

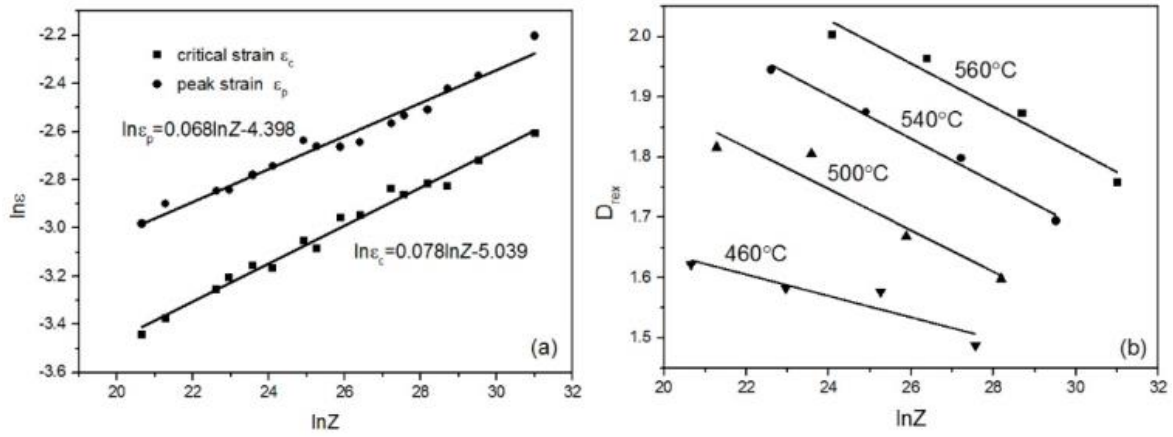

(a)lnε_{p} versus ln$Z$ and lnε_{c} versus ln$Z$ plot;(b) ln$D$ versus ln$Z$

Figure 7. The relationships betweenε_{p}, ε_{c}, $\mathrm{D_{drex}}$ and Z

$$\varepsilon_{\mathrm{p}} = 1.2 \times 10^{-2} \mathrm{Z}^{0.069} \tag{10}$$

$$\varepsilon_{\mathrm{c}} = 7.5 \times 10^{-3} \mathrm{Z}^{0.073} \tag{11}$$

$$\varepsilon_{\mathrm{c}}/\varepsilon_{\mathrm{p}} \approx (0.678\sim0.707) \tag{12}$$

$$\mathrm{D_{drex}} = 12.89 \mathrm{Z}^{0.03} \tag{13}$$

3.5. Dynamic recrystallization kinetics

The volume fraction of dynamic recrystallization could be described with Avrami type as follows [12]:

$$\mathrm{X_{DRX}} = 1 - \exp\left[-0.693\left(\frac{\varepsilon-\varepsilon_{\mathrm{c}}}{\varepsilon_{0.5}}\right)^2\right] \tag{14}$$

$$\mathrm{X_{DRX}} = \frac{\sigma_{\mathrm{p}}-\sigma}{\sigma_{\mathrm{p}}-\sigma_{\mathrm{s}}} \tag{15}$$

Where, X_{DRX} is dynamic recrystallization fraction, ε the true strain, ε_c the critical strain for the onset of DRX; $\varepsilon_{0.5}$ is the strain that corresponds to the DRX fraction 50%;σ_{p} the peak stress; σ the flow stress; σ_{s} the stress in steady state;

According to the equation, when the X_{DRX} is 50%, flow stress is confirmed. The strain corresponding to the flow stress is $\varepsilon_{0.5}$.

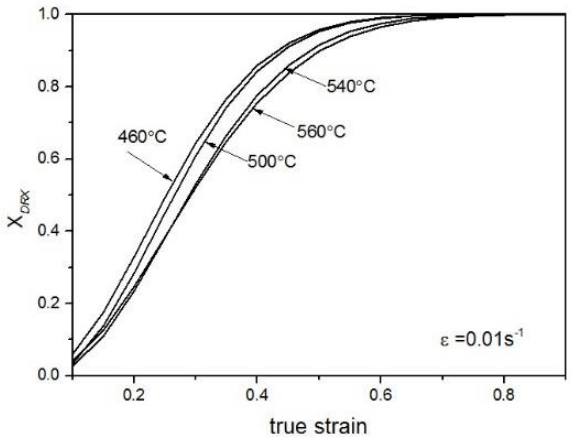

Figure 8. Predicted dynamic recrystallization fraction by model at different temperatures.

Figure 8 shows the trend of DRX fraction with the true strain .It is seen that the fraction is decreased when the temperatures increase under the same strain. The true strain will increase when the temperatures increase under the same DRX fraction

4. Conclusions

The dynamic recrystallization behavior of 6082 Al-Si-Mg aluminum alloy is investigated by compression experiment in high temperature. The main results can be summarized as follows:

(1) At lower strain rates, hardening and softening due to dynamic recrystallization are in balance; at high strain rates, hardening and softening due to dynamic recrystallization alternately dominated.

(2) The deformation activation energy of 6082 Al-Si-Mg is about 174.9 kJ $\cdot$ mol^{-1}.

(3) Lower strain rates are beneficial to increase the volume fraction of DRX, the average grain size is coarse; High strain rates are beneficial to refine average grain size, the volume fraction of DRX is less than that in low strain rates. High temperature cause coarse grains.

(4) The relationship between DRX grain size D_{drex} of dynamic recrystallization and Zenner-Hollomon parameter Z: $D_{\mathrm{drex}}=12.89Z^{0.03}$.

(5) The kinetics model of volume fraction of dynamic recrystallization can be used to predict the trend of DRX

5. Reference

[1] Ebrahimi G R, Keshmiri, Maldar A R and Momeni A 2012 *Mater. Sci. Technol* **28** 467-73
[2] Poliak E I and Jonas J J 1996 *Acta mater* **44** 127-36
[3] Sellars 1981 *Metals Forum* **4** 75
[4] Poliak E I and Jonas J J 2003 *ISIJ International* **43** 684-691
[5] Guo H L, Sun Z C and Yang H 2013 *The Chinese Journal of Nonferrous Metals* **6** 1507-14
[6] Chen X H, Chen K H and Yang P X 2013 *The Chinese Journal of Nonferrous Metals* **1** 44-50
[7] Shi L, Yang H and Guo G 2014 *Journal of Plasticity Engineering* **1** 65-70
[8] Feng D, Zhang X M and Liu S D and Deng Y L 2014 *Mater. Sci. Eng. A* **608** 63-72
[9] Mirzadeh H and Najafizadeh A 2010 *Materials and Design* **31** 1174-79
[10] Zenner C and Hollmon J H 1944 *Journal of Applied Physics* **22** 22-32
[11] Robert M 1983 *The international Journal of Robotics Research* **2** 50-72
[12] Shanban M, Eghbali B 2010 *Mater. sci. Eng. A* **527** 4320-5